

1

## 2 **<sup>19</sup>F labelled Glycosaminoglycan Probes for Solution NMR and Non-linear (CARS)** 3 **Microscopy**

4 Marcelo A. Lima<sup>1,2</sup>, Renan P. Cavalheiro<sup>1</sup>, Gustavo M.Viana<sup>1</sup>, Maria C.Z. Meneghetti<sup>1</sup>, Timothy  
5 R. Rudd<sup>3,2</sup>, Mark A. Skidmore<sup>4</sup>, Andrew K. Powell<sup>5,2</sup> and Edwin A. Yates<sup>2,1,4\*</sup>

6 1. *Department of Biochemistry, UNIFESP, Rua Três de Maio, Vila Clementino, São Paulo, 40440-SP Brazil*

7 2. *Department of Biochemistry, University of Liverpool, Liverpool L69 7ZB United Kingdom*

8 3. *The National Institute of Biological Standards and Controls, Blanche Lane, South Mimms, Potters Bar,*  
9 *Hertfordshire EN6 3QG United Kingdom*

10 4. *School of Life Sciences, Keele University, Staffordshire ST5 5BG United Kingdom*

11 5. *School of Pharmacy and Biomolecular Sciences, Liverpool John Moores University, Liverpool L3 3AF United*  
12 *Kingdom*

13 \*Correspondence to [eyates@liv.ac.uk](mailto:eyates@liv.ac.uk)

14

### 15 **Abstract**

16 **Studying polysaccharide-protein interactions under physiological conditions by**  
17 **conventional techniques is challenging. Ideally, macromolecules could be followed by both**  
18 ***in vitro* spectroscopy experiments as well as in tissues using microscopy, to enable a**  
19 **proper comparison of results over these different scales but, often, this is not feasible. The**  
20 **cell surface and extracellular matrix polysaccharides, glycosaminoglycans (GAGs) lack**  
21 **groups that can be detected selectively in the biological milieu. The introduction of <sup>19</sup>F**  
22 **labels into GAG polysaccharides is explored and the interaction of a labelled GAG with the**  
23 **heparin-binding protein, antithrombin, employing <sup>19</sup>F NMR spectroscopy is followed.**  
24 **Furthermore, the ability of <sup>19</sup>F labelled GAGs to be imaged using CARS microscopy is**  
25 **demonstrated. <sup>19</sup>F labelled GAGs enable both <sup>19</sup>F NMR protein-GAG binding studies in**  
26 **solution at the molecular level and non-linear microscopy at a microscopic scale to be**  
27 **conducted on the same material, essentially free of background signals.**

28 **Key words: Heparin, NMR, <sup>19</sup>F, Non-linear microscopy**

29

### 30 **Introduction**

31 An understanding of the biological processes that determine cell-cell signalling, hence coordinate  
32 cellular responses and maintain healthy growth and development, must encompass a detailed  
33 appreciation of interactions between proteins and extracellular matrix (ECM) polysaccharides [1-3].  
34 Moreover, the network of interactions that defines healthy homeostasis is also relevant to disease  
35 processes, many of which involve some modification to this network [1]. One practical challenge is  
36 how to study phenomena, particularly interactions, that correlate with natural or disease processes,  
37 but which range in scale from the dimensions of molecules to the macroscopic level of tissues and  
38 organisms. Current approaches at the molecular level include spectroscopic and crystallographic  
39 techniques, which allow investigation at the level of ensembles of molecules, while various forms of  
40 (mainly) optical microscopy allow tissues to be examined in detail at the macroscopic level.  
41 However, few techniques or tools have the ability to work across these scales. Each approach also  
42 tends to employ distinct and largely incompatible labelling procedures and detection techniques,  
43 hence, it can be difficult to interpret them together, or extrapolate results from one technique to the  
44 other and, consequently, to relate the observations to the biological processes under investigation.  
45 Clearly, it would be advantageous if it were possible to utilise the same materials throughout.

46 Studying interactions between proteins and polysaccharides in solution presents a number  
47 of further challenges. There are several reasons why conventional techniques for the detailed  
48 study of proteins, either in the solid state employing crystallography, or in solution using NMR, are  
49 often unsuitable when the protein to be studied is bound to a polysaccharide ligand. First, it is not  
50 usually possible to crystallise a protein in the presence of a polysaccharide and, especially in the  
51 case of extracellular polysaccharides such as the glycosaminoglycans (GAGs), the polysaccharide  
52 is frequently a complex and heterogeneous mixture of sequences and chain dimensions. The  
53 problem has been managed in several crystallographic and NMR studies by employing short  
54 oligosaccharide fragments acting as proxies for their parent polysaccharide and this has revealed  
55 some structural details of their interactions [4-7]. The use of oligosaccharide fragments as a stand-  
56 in for the polysaccharide is widespread, although there are differences in binding properties which  
57 have their origins in the distinct conformational and motional behaviour of oligo- compared to  
58 polysaccharides but, possibly, also in the different numbers of potential binding sites in the two  
59 cases [8]. In the case of  $^1\text{H}$  and  $^{13}\text{C}$  NMR, the size and low mobility of protein-polysaccharide  
60 complexes in solution can lead to line broadening. Additional techniques with which to follow the  
61 interactions between proteins and GAGs are therefore required. One possibility is solid state NMR,  
62 which has been used to obtain detailed information in aggregates consisting of peptides and GAGs  
63 [9,10] but, it would also be desirable to be able to follow the location of GAGs in tissues by  
64 microscopy. One family of emerging techniques, based on Raman Spectroscopy, involves the  
65 selective observation of chemical groups that are particular to the molecules of interest.  
66 Unfortunately, there are no obvious Raman signals which are unique to GAGs. Their characteristic  
67 carboxylate, amine, acetyl and sulfate groups are also present to some extent in other biological  
68 molecules. With these considerations in mind, we have sought a label which has desirable  
69 characteristics both in terms of sensitivity in microscopy and NMR, exhibits very low or no  
70 background signal in biological systems and that can be informative as regards changes in its  
71 environment. The  $^{19}\text{F}$  nucleus fulfils many of these criteria and here, we investigate the possibility  
72 of employing  $^{19}\text{F}$  labelling of GAG poly- and oligosaccharides as a route to unambiguous  
73 information concerning protein-polysaccharide interactions using NMR spectroscopy, and as a  
74 potential means of following events in tissues employing non-linear (CARS) microscopy.

75 The  $^{19}\text{F}$  nucleus constitutes 100% of the fluorine occurring naturally and, with nuclear spin  
76  $\frac{1}{2}$ , presents readily-interpretable NMR signals, which are sensitive to the surrounding chemical  
77 environment owing to the lone pair electrons in the outer shell of the  $^{19}\text{F}$  atom. A strong  
78 paramagnetic component dominates the chemical shift and, usefully, also provides good signal  
79 dispersion.  $^{19}\text{F}$  NMR spectra in biological systems are very clean since almost no  $^{19}\text{F}$  is present in  
80 biology naturally [11] and is particularly useful in systems whose size, immobility and/or complexity  
81 precludes conventional NMR approaches, such as transmembrane proteins and macromolecular  
82 complexes. The sensitivity of the  $^{19}\text{F}$  nucleus to its immediate environment, including to solvent  
83 water or deuterium oxide (in  $\text{D}_2\text{O}$  compared to  $\text{D}_2\text{O}/\text{H}_2\text{O}$  80:20, v/v,  $\Delta\delta = 0.13$  ppm), also makes it  
84 suitable for studies involving site-specific labelling, denaturation experiments [12] and for  
85 identifying interactions at protein interfaces. In addition, the temperature dependence of  $^{19}\text{F}$  NMR  
86 signal line widths renders it sensitive to mobility, from which information relating to both binding  
87 and stability can be deduced. Although not investigated here, the chemistry employed to introduce  
88  $^{19}\text{F}$  into biomolecules is also suitable for  $^{18}\text{F}$ , opening-up the possibility of conducting positron  
89 emission tomography (PET). Labelling of proteins with  $^{18}\text{F}$  [13], as well as of sugars during their  
90 chemical synthesis has been reported [14,15] and the chemical labelling of amino acid side chains  
91 with fluorine via a range of amino acid side chains (aliphatic, aromatic and cysteine) has also been  
92 achieved [16]. Such labels can have effects on the structure of the protein however, and one  
93 approach that has been explored to minimise this problem is to conduct partial substitution [17,18].

94 The attachment of suitable  $^{19}\text{F}$  containing groups to glycosaminoglycan (GAG)  
95 polysaccharides would extend many of the advantages exploited for proteins to the GAG class of  
96 molecules, thereby opening-up the study of polysaccharide-protein interactions. The choice of label  
97 made here; *N*-trifluoroacetyl, which is readily introduced to free amino groups of glucosamine  
98 residues within the polysaccharide chains, and trifluoroalkylamines, (either 2,2,2-  
99 trifluoroethylamine (TFEA) or 3,3,3 trifluoropropylamine (TFPA)), which can be introduced through  
100 amide formation onto the former carboxylate groups of uronic acids via the 1-ethyl-3-(3-  
101 dimethylaminopropyl) carbodiimide (EDC)-activated ester, both contain a terminal  $-\text{CF}_3$  group.  
102 These provide a clean signal in  $^{19}\text{F}$  NMR, owing to short  $T_1$  relaxation times and low chemical shift  
103 anisotropy but, usefully, also provide distinct Raman transitions, exploitable in coherent Anti-  
104 Stokes Raman Scattering (CARS) and other, non-linear microscopy techniques. Signals arising  
105 from C-F bond stretching are also unambiguous, there being effectively no background signals.  
106 Labelling GAG macromolecules with  $^{19}\text{F}$  using  $-\text{CF}_3$  groups can therefore provide both a suitable  
107 NMR signal with favourable spectroscopic properties capable of providing information regarding  
108 molecular interactions *in vitro*, but also in tissues [12], as well as a signal that can be used in non-  
109 linear microscopy (such as CARS), which is free of background and interference from water,  
110 allowing direct chemical imaging. Two straightforward methods of introducing  $^{19}\text{F}$  into GAG  
111 polysaccharides (denoted (i) and (ii) below) are reported. Illustrative examples of their use as  
112 probes of molecular interactions in solution using  $^{19}\text{F}$  NMR spectroscopy and the ability to image  
113 them using CARS microscopy are demonstrated.

## 114 **Methods**

115 (i) Preparation of trifluoroacetylated glycosaminoglycan polysaccharides (1):- The first procedure is  
116 based on *O*-acylation using acetic anhydride, in which iodine has been proposed to act as a Lewis  
117 acid catalyst [19]. The free amino groups of glucosamine residues in heparin (used widely as an  
118 experimental proxy for the more scarce, naturally occurring ligand, heparan sulfate) polysaccharide  
119 derivatives, in which free amino groups had been introduced [20], was labelled selectively using  
120 trifluoroacetic anhydride with iodine as catalyst. With this class of large, anionic polysaccharides,  
121 however, the reaction was found to be highly selective for the free amino groups of the  
122 glucosamine residues of the polysaccharides, forming trifluoroacetamido-derivatives. De-N-  
123 sulfated heparin polysaccharide (25 mg,  $\sim 40$   $\mu\text{mol}$  of disaccharide equivalents) was added as a  
124 solid to trifluoroacetic anhydride (9.5 mmol), with solid iodine flakes (0.2 mmol) and stirred at room  
125 temperature. The reactants were then precipitated in ice-cold ethanol (200 mL) and filtered,  
126 washed with ethanol, any large iodine grains were removed and the filtrate was washed until any  
127 remaining iodine had been removed (brown colour subsides: *n.b.* iodine in the wash was  
128 neutralised by the addition of solid sodium metabisulfite until a clear iodide containing solution had  
129 been obtained and was then disposed of). The recovered GAG compounds; *N*-trifluoroacetyl  
130 heparin (**1**) was dialysed (7 kDa cut-off dialysis membrane (SpectraPore, USA)) 3 times against 2  
131 L of distilled water, the dialysate was recovered, then subjected to gel permeation chromatography  
132 (Sephadex G-25) and characterised by  $^{19}\text{F}$  [Table 1] and  $^{13}\text{C}$  NMR spectroscopy [Supp. Fig. 1]  
133 prior to being employed in experiments.

134 (ii) Introduction of trifluoroalkyl groups at carboxylate groups of uronic acids of heparin and the  
135 heparin-derived pentasaccharide, Arixtra<sup>TM</sup>, via EDC activation (2), (3) and (4):- The second  
136 method involved attachment of the  $^{19}\text{F}$  label via the carboxylate groups of uronate residues in  
137 GAGs. The carboxylate groups were activated using 1-ethyl-3-(3-dimethylaminopropyl)  
138 carbodiimide (EDC, Pearce) in 50 mM HEPES buffer and the resulting EDC ester reacted with an  
139 alkylamine; either 2,2,2 trifluoroethylamine (TFEA) or 3,3,3 trifluoropropylamine (TFPA), both  
140 convenient water soluble fluoroamines, of moderate volatility (b.p. 36-37 and 67.5-68  $^\circ\text{C}$   
141 respectively), to form the corresponding fluoroamides. [Note: - If EDC is added before the

142 alkylamine to the GAG solution, a side-product persists, evident in  $^{13}\text{C}$  and  $^1\text{H}$  NMR, thought to  
143 originate from a rearrangement of the isourea adduct [21]. This provides an alternative labelling  
144 method, acting specifically on the carboxylate groups of the uronic acids. The method was applied  
145 to both GAG polysaccharides (described in (a) below) and to the pentasaccharide antithrombotic  
146 drug Arixtra<sup>TM</sup>, whose systematic name, [ $\alpha$ -D-Glucopyranoside, methyl O-2- deoxy-6-O-sulfo-2-  
147 (sulfoamino) - $\alpha$ -D-glucopyranosyl-(1 $\rightarrow$ 4)-O- $\beta$ -D-glucopyranuronosyl-(1 $\rightarrow$ 4)-O-2-deoxy-3,6-di-O-  
148 sulfo -2-(sulfoamino)- $\alpha$ -D-glucopyranosyl-(1 $\rightarrow$ 4)- O-2-O-sulfo- $\alpha$ -L- idopyranuronosyl- (1 $\rightarrow$ 4) -2-  
149 deoxy-2-(sulfoamino)-6-(hydrogen sulfate), sodium salt], is abbreviated to 'AGAIA', and described  
150 in (b).

151 (a). Derivatisation of Ido-2-de-sulfated heparin and heparin with TFEA (2) and (3):- The ido-2-de-O-  
152 sulfated porcine mucosal heparin<sup>20</sup> (for the preparation of (2)) or porcine mucosal heparin (for the  
153 preparation of (3)) (25 mg) was dissolved in 50 mM HEPES buffer (0.50 mL, pH 6.8), TFEA (61  
154  $\mu\text{mol}$ ) added, followed by EDC (26  $\mu\text{mol}$ ). The reaction mixture was then stirred at room  
155 temperature (30 mins) and the products ((2) or (3)) were dialysed (7 kDa cut-off dialysis membrane  
156 (SpectraPore, USA)) 3 times against 2 L of distilled water, the dialysate recovered, subjected to gel  
157 permeation chromatography (Sephadex G-25) and employed in experiments.

158  
159 (b). Derivatisation of AGAIA pentasaccharide with TFPA (4):- The pentasaccharide, AGAIA  
160 (Arixtra<sup>TM</sup>) (2.5. mg, 1.7  $\mu\text{mol}$  in 0.5 mL 137 mM NaCl) was mixed with HEPES buffer (0.5 mL, 50  
161 mM, pH 6.8) and TFPA (2  $\mu\text{L}$ , 22  $\mu\text{mol}$ ) were added, followed by EDC (1 mg, 5.2  $\mu\text{mol}$ ) and shaken  
162 for 10 mins at room temperature. The products were then desalted by gel permeation  
163 chromatography using Sephadex G-25, freeze dried and characterised by  $^{19}\text{F}$  NMR (**Table 1**)  
164 before being employed in binding experiments.

165  
166 (iii).  $^{19}\text{F}$  NMR investigation of GAG interaction with antithrombin in solution:- Decoupled  $^{19}\text{F}$  NMR  
167 experiments were conducted on a Bruker Avance III 500 MHz spectrometer (UNICAMP, Instituto  
168 de Quimica, Campinas, Brazil) using antithrombin (AT; 100  $\mu\text{L}$ , 15 mg/mL in PBS containing  $\text{D}_2\text{O}$ )  
169 and additions of (4), (500  $\mu\text{L}$ , 1 mg/mL) or heparin (500  $\mu\text{L}$ , 5 mg/mL) [**Fig. 1**].

170 (iv). Selective Detection of  $^{19}\text{F}$  labelled heparin-derived polysaccharides using Non-linear (CARS)  
171 Microscopy:- The form of Raman microscopy used here is based on a non-linear Raman technique  
172 termed coherent anti-Stokes Raman scattering (CARS). This technique can generate coherent  
173 signals up to  $10^5$  times stronger than conventional Raman and relies on the use of light as a pump  
174 to alter the populations of vibrational states, then to probe, providing anti-Stokes light emission of  
175 higher energy (i.e. lower wavelength) than that of the pump [22]. The  $^{19}\text{F}$  labelled heparin  
176 derivatives (1) to (3) were used in CARS Raman microscopy experiments, in which the Raman  
177 signal from the  $\text{CF}_3$  group provided a means of detecting selectively a film of the polysaccharide by  
178 means of its CARS signal [**Fig. 2**].

## 179 **Results and Discussion**

180 The fluorinated products were first characterised by  $^{19}\text{F}$  NMR to provide a range of  
181 complementary probes, suitable for GAG-protein interactions studies and non-linear spectroscopy  
182 [**Table 1**]. The reaction was also applied to the antithrombin (AT) binding pentasaccharide,  
183 (AGAIA) and was found, surprisingly, to label selectively the GlcA carboxylate group [**Supp. Fig.**  
184 **2**]. This product was then shown by  $^{19}\text{F}$  NMR spectroscopy to bind AT in solution [**Fig. 1A**; lower  
185 panel (unbound) and middle panel (bound)] by virtue of a change in chemical shift position  
186 downfield of unreacted TFPA and binding was confirmed using fluorescence shift assay [**Fig. 1B**].



187 The binding of (4) to AT in solution was then disrupted by the addition of excess unlabelled heparin  
188 [Fig. 1A; upper panel]. Furthermore, the <sup>19</sup>F labelled AGAIA pentasaccharide was able to stabilise  
189 AT to an extent comparable to the unmodified form [Fig. 1B] confirming its interaction with  
190 antithrombin [23].

191 Images (1.16 mm x 1.16 mm) were recorded in the forward CARS (F-CARS) mode on a  
192 Leica TSC-SP8 CARS instrument (Wetzler, Germany), employing pump lasers (the first pump  
193 laser selected at 928.2 nm and the second CARS laser, fixed, at 1064.5 nm) both at 46 % power.  
194 Images, detected at 1379 cm<sup>-1</sup> pre-determined to offer useful C-F derived Raman signals [23] were  
195 recorded at 0.05 frames/s with 1.20 μs dwell time per pixel, a gain of 850.82 V and at 10 x  
196 magnification. Five μL of compounds (1), (2) and (3) were dried from solutions (1 mg/mL in H<sub>2</sub>O)  
197 on a glass slide and imaged [Fig. 2A, 2B and 2C]. As a control, the second laser (1064.5 nm) was  
198 then switched-off and no image was observed, confirming that the images were CARS-derived  
199 (Fig. 2D).

200 Both methods of labelling heparin and other GAG derivatives are suitable for conducting NMR and  
201 microscopy studies and this will allow the same reagent to be used to examine events on scales  
202 ranging from those of molecules to tissues, providing more readily interpretable data. There are  
203 many other types of selective labelling that could be exploited to allow <sup>19</sup>F NMR and non-linear  
204 microscopy with other classes of macromolecules, such as proteins. One example would be to  
205 incorporate <sup>19</sup>F labelled Trp residues, which can be achieved biosynthetically through either 5- or  
206 6- fluorouridine. In this way, it will also be possible to follow proteins in tissues and the GAG  
207 polysaccharides with which they interact, as well as to study exactly the same interactions *in vitro*  
208 using <sup>19</sup>F NMR. One interesting finding was that, in contrast to the situation observed for heparin  
209 polysaccharides, the reaction of TFPA with the pentasaccharide, AGAIA, did provide highly  
210 selective reaction with the carboxylate group of the GlcA residue over those of IdoA [Supp. Fig. 2]  
211 perhaps reflecting its more accessible, equatorial conformation. The use of CARS microscopy to  
212 study molecular interactions in tissues is in its infancy but, promises to be able to investigate  
213 complex assemblies by virtue of its ability to selectively observe a range of chemical groups,  
214 whether they be naturally occurring, or have been introduced deliberately. This paper proposes a  
215 number of <sup>19</sup>F-labelled GAG probes which can also be used in both NMR and CARS microscopy  
216 applications.

217

## 218 Acknowledgements

219 MAL and EAY gratefully acknowledge Coordenação de Aperfeiçoamento de Pessoal de Nível  
220 Superior (CAPES), Fundação de Amparo à Pesquisa do Estado de São Paulo (FAPESP) and  
221 Conselho Nacional de Desenvolvimento Científico e Tecnológico (CNPq) for financial support. The  
222 authors also gratefully acknowledge Dr Tony Curtis of Keele University for the provision of <sup>19</sup>F  
223 NMR spectra. Dr Andrew V. Stachulski of the Department of Chemistry, University of Liverpool is  
224 thanked for useful discussions and advice. The authors also thank Dr. Claudio Tormena of  
225 University of Campinas (UNICAMP), Brazil for provision of NMR facilities.

226

227

228

229

231 **References**

- 232 1. Ori, A., Wilkinson, M.C., Fernig, D.G.: A systems biology approach for the investigation of the  
233 heparin/heparan sulfate interactome. *The Journal of biological chemistry* **286**(22), 19892-  
234 19904 (2011). doi:10.1074/jbc.M111.228114
- 235 2. Solari, V., Borriello, L., Turcatel, G., Shimada, H., Sposto, R., Fernandez, G.E., Asgharzadeh, S.,  
236 Yates, E.A., Turnbull, J.E., DeClerck, Y.A.: MYCN-dependent expression of sulfatase-2  
237 regulates neuroblastoma cell survival. *Cancer research* **74**(21), 5999-6009 (2014).  
238 doi:10.1158/0008-5472.CAN-13-2513
- 239 3. Xu, R., Rudd, T.R., Hughes, A.J., Siligardi, G., Fernig, D.G., Yates, E.A.: Analysis of the  
240 fibroblast growth factor receptor (FGFR) signalling network with heparin as coreceptor:  
241 evidence for the expansion of the core FGFR signalling network. *The FEBS journal*  
242 **280**(10), 2260-2270 (2013). doi:10.1111/febs.12201
- 243 4. Guerrini, M., Elli, S., Mourier, P., Rudd, T.R., Gaudesi, D., Casu, B., Boudier, C., Torri, G.,  
244 Viskov, C.: An unusual antithrombin-binding heparin octasaccharide with an additional 3-  
245 O-sulfated glucosamine in the active pentasaccharide sequence. *The Biochemical journal*  
246 **449**(2), 343-351 (2013). doi:10.1042/BJ20121309
- 247 5. Guglier, S., Hricovini, M., Raman, R., Polito, L., Torri, G., Casu, B., Sasisekharan, R., Guerrini,  
248 M.: Minimum FGF2 binding structural requirements of heparin and heparan sulfate  
249 oligosaccharides as determined by NMR spectroscopy. *Biochemistry* **47**(52), 13862-13869  
250 (2008).
- 251 6. Viskov, C., Elli, S., Urso, E., Gaudesi, D., Mourier, P., Herman, F., Boudier, C., Casu, B., Torri,  
252 G., Guerrini, M.: Heparin dodecasaccharide containing two antithrombin-binding  
253 pentasaccharides: structural features and biological properties. *The Journal of biological*  
254 *chemistry* **288**(36), 25895-25907 (2013). doi:10.1074/jbc.M113.485268
- 255 7. Wei, Z., Deakin, J.A., Blaum, B.S., Uhrin, D., Gallagher, J.T., Lyon, M.: Preparation of  
256 heparin/heparan sulfate oligosaccharides with internal N-unsubstituted glucosamine residues  
257 for functional studies. *Glycoconjugate journal* **28**(8-9), 525-535 (2011).  
258 doi:10.1007/s10719-011-9352-3
- 259 8. Powell, A.K., Yates, E.A., Fernig, D.G., Turnbull, J.E.: Interactions of heparin/heparan sulfate  
260 with proteins: appraisal of structural factors and experimental approaches. *Glycobiology*  
261 **14**(4), 17R-30R (2004). doi:10.1093/glycob/cwh051
- 262 9. Madine, J., Clayton, J.C., Yates, E.A., Middleton, D.A.: Exploiting a (13)C-labelled heparin  
263 analogue for in situ solid-state NMR investigations of peptide-glycan interactions within  
264 amyloid fibrils. *Organic & biomolecular chemistry* **7**(11), 2414-2420 (2009).  
265 doi:10.1039/b820808e
- 266 10. Madine, J., Pandya, M.J., Hicks, M.R., Rodger, A., Yates, E.A., Radford, S.E., Middleton,  
267 D.A.: Site-specific identification of an abeta fibril-heparin interaction site by using solid-  
268 state NMR spectroscopy. *Angewandte Chemie* **51**(52), 13140-13143 (2012).  
269 doi:10.1002/anie.201204459
- 270 11. Danielson, M.A., Falke, J.J.: Use of 19F NMR to probe protein structure and conformational  
271 changes. *Annual review of biophysics and biomolecular structure* **25**, 163-195 (1996).  
272 doi:10.1146/annurev.bb.25.060196.001115
- 273 12. Feeney, J., McCormick, J.E., Bauer, C.J., Birdsall, B., Moody, C.M., Starkmann, B.A., Young,  
274 D.W., Francis, P., Havlin, R.H., Arnold, W.D., Oldfield, E.: 19F Nuclear Magnetic  
275 Resonance Chemical Shifts of Fluorine Containing Aliphatic Amino Acids in Proteins:  
276 Studies on *Lactobacillus casei* Dihydrofolate Reductase Containing (2S,4S)-5-  
277 Fluoroleucine. *Journal of the American Chemical Society* **118**(36), 8700-8706 (1996).  
278 doi:10.1021/ja960465i
- 279 13. Chang, Y.S., Jeong, J.M., Lee, Y.S., Kim, H.W., Rai, G.B., Lee, S.J., Lee, D.S., Chung, J.K.,  
280 Lee, M.C.: Preparation of 18F-human serum albumin: a simple and efficient protein labeling

- 281 method with  $^{18}\text{F}$  using a hydrazone-formation method. *Bioconjugate chemistry* **16**(5),  
282 1329-1333 (2005). doi:10.1021/bc050086r
- 283 14. Boutureira, O., D'Hooge, F., Fernandez-Gonzalez, M., Bernardes, G.J., Sanchez-Navarro, M.,  
284 Koeppe, J.R., Davis, B.G.: Fluoroglycoproteins: ready chemical site-selective incorporation  
285 of fluorosugars into proteins. *Chemical communications* **46**(43), 8142-8144 (2010).  
286 doi:10.1039/c0cc01576h
- 287 15. Boutureira, O., Rodriguez, M.A., Diaz, Y., Matheu, M.I., Castillon, S.: Studies on the Zn(II)-  
288 mediated electrophilic selenocyclization and elimination of 3,4-O-isopropylidene-protected  
289 hydroxyalkenyl sulfides: synthesis of a 2-phenylselenenyl glycol. *Carbohydrate research*  
290 **345**(8), 1041-1045 (2010). doi:10.1016/j.carres.2010.03.001
- 291 16. Klein-Seetharaman, J., Getmanova, E.V., Loewen, M.C., Reeves, P.J., Khorana, H.G.: NMR  
292 spectroscopy in studies of light-induced structural changes in mammalian rhodopsin:  
293 applicability of solution ( $^{19}\text{F}$ ) NMR. *Proceedings of the National Academy of Sciences of*  
294 *the United States of America* **96**(24), 13744-13749 (1999).
- 295 17. Kitevski-LeBlanc, J.L., Evancics, F., Scott Prosser, R.: Optimizing ( $^{19}\text{F}$ ) NMR protein  
296 spectroscopy by fractional biosynthetic labeling. *Journal of biomolecular NMR* **48**(2), 113-  
297 121 (2010). doi:10.1007/s10858-010-9443-7
- 298 18. Kitevski-Leblanc, J.L., Hoang, J., Thach, W., Larda, S.T., Prosser, R.S.: ( $^{19}\text{F}$ ) NMR studies  
299 of a desolvated near-native protein folding intermediate. *Biochemistry* **52**(34), 5780-5789  
300 (2013). doi:10.1021/bi4010057
- 301 19. Ravindranathan, A., Parks, T.N., Rao, M.S.: New isoforms of the chick glutamate receptor  
302 subunit GluR4: molecular cloning, regional expression and developmental analysis. *Brain*  
303 *research. Molecular brain research* **50**(1-2), 143-153 (1997).
- 304 20. Yates, E.A., Santini, F., Guerrini, M., Naggi, A., Torri, G., Casu, B.:  $^1\text{H}$  and  $^{13}\text{C}$  NMR spectral  
305 assignments of the major sequences of twelve systematically modified heparin derivatives.  
306 *Carbohydrate research* **294**, 15-27 (1996).
- 307 21. 3.5 Carbodiimides. In: Felix, A., Moroder, L., Toniolo, C. (eds.) *Houben-Weyl Methods of*  
308 *Organic Chemistry Vol. E 22a, 4th Edition Supplement, vol. E 22 a. Methoden der*  
309 *Organischen Chemie (Houben-Weyl)*. Georg Thieme Verlag, Stuttgart, (2004)
- 310 22. Maker, P.D., Terhune, R.W.: Study of Optical Effects Due to an Induced Polarization Third  
311 Order in the Electric Field Strength. *Physical Review* **137**(3A), A801-A818 (1965).
- 312 23. Chaffin, J.C.T., Marshall, T.L.: Using a gas cell to characterize FT-IR air sensor performance.  
313 In: 1999, pp. 69-78

314

315

316

317

318

319

320

321

322

323

324

325 **Figures and Tables**

326

327

328

329

330

331

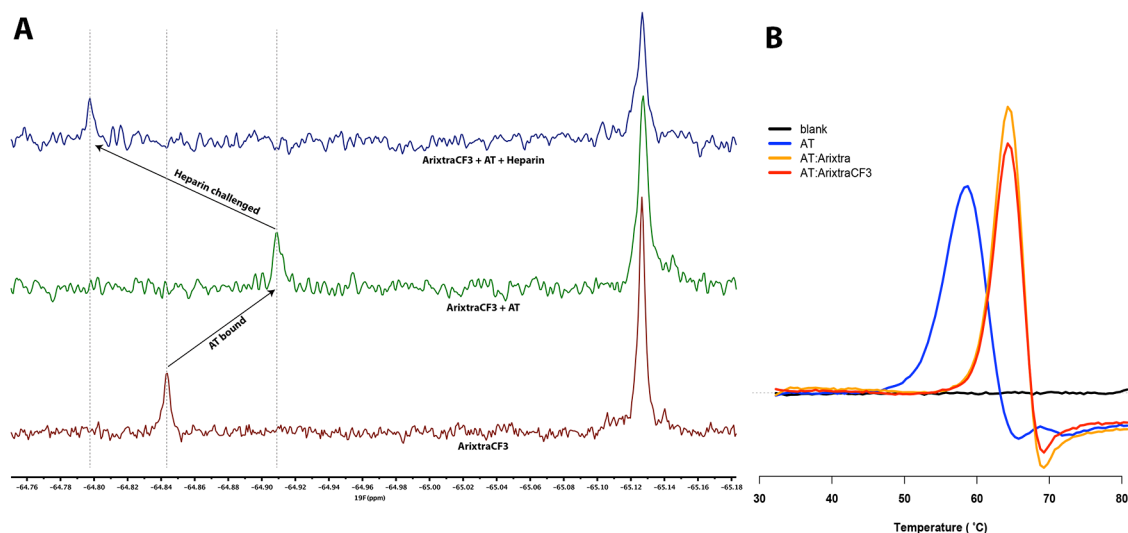
332

333

334

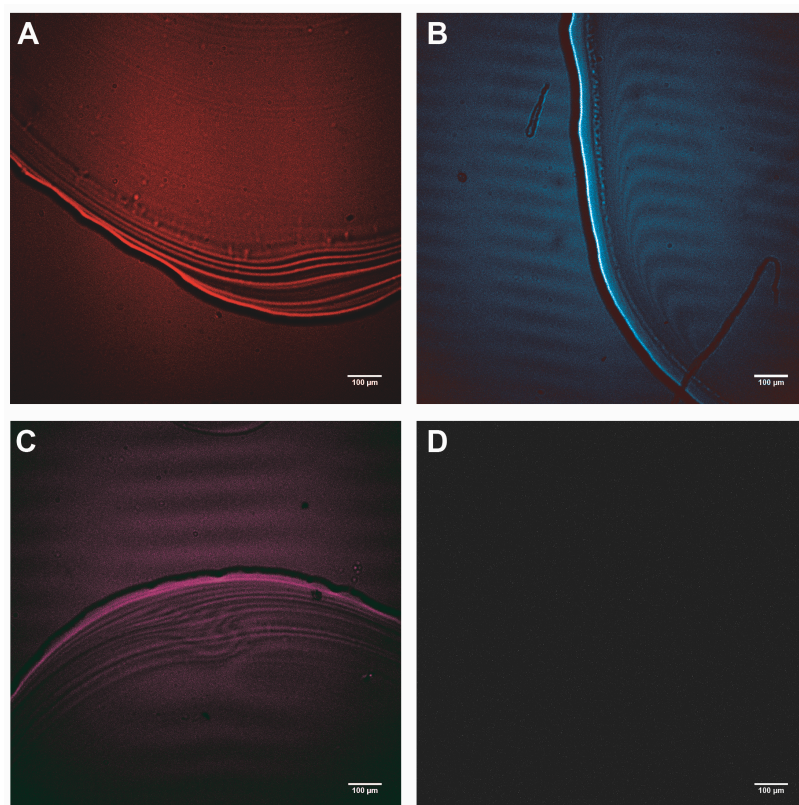
335

336



337 **Figure 1.  $^{19}\text{F}$  labelled GAGs can be used as probes of protein binding and of solution**  
338 **environment.  $^{19}\text{F}$  NMR spectra of: A. (lower)  $^{19}\text{F}$ -labelled AGAIA pentasaccharide (4) alone,**  
339 **(middle) bound  $^{19}\text{F}$ -labelled AGAIA pentasaccharide in the presence of antithrombin (AT) and  $^{19}\text{F}$ -**  
340 **labelled AGAIA pentasaccharide in the presence of antithrombin plus added heparin to compete-**  
341 **off the ligand, (upper) returning to a distinct chemical shift position, demonstrating the sensitivity of**  
342 **the  $^{19}\text{F}$  label to the solution environment. B. Differential scanning fluorimetry showing that the  $^{19}\text{F}$**   
343 **labelled AGAIA pentasaccharide (4) stabilised AT (red curve, compared to AT alone, blue curve)**  
344 **to an extent comparable to the unlabelled pentasaccharide (gold curve).**

345



358  
359

360 **Figure 2. CARS images of dried films of  $^{19}\text{F}$  labelled GAG (heparin) derivatives. A.** Compound  
361 **(1), B.** Compound (2), **C.** Compound (3), **D.** Control experiment with the 1064.5 nm CARS laser  
362 switched-off, showing no image and confirming that the images in **A-C** are derived from CARS.  
363 Images were recorded at 10 x magnification and correspond to a field size of 1.16 mm x 1.16 mm.

364

365 **Table 1.**  $^{19}\text{F}$  NMR chemical shifts for (1) to (4).

366

367

Name	Compound	$\delta^{19}\text{F}$ /ppm
<i>N</i> -Trifluoroacetyl porcine mucosal heparin	(1)	-75.58 <sup>a</sup>
Trifluoroethylamido-Ido-2-de- <i>O</i> -sulfated heparin	(2)	-72.2 <sup>a</sup>
Trifluoroethylamido-heparin	(3)	-72.3 <sup>a</sup>
AGAIA (Arixtra <sup>TM</sup> pentasaccharide)	(4)	-64.8 <sup>b</sup>

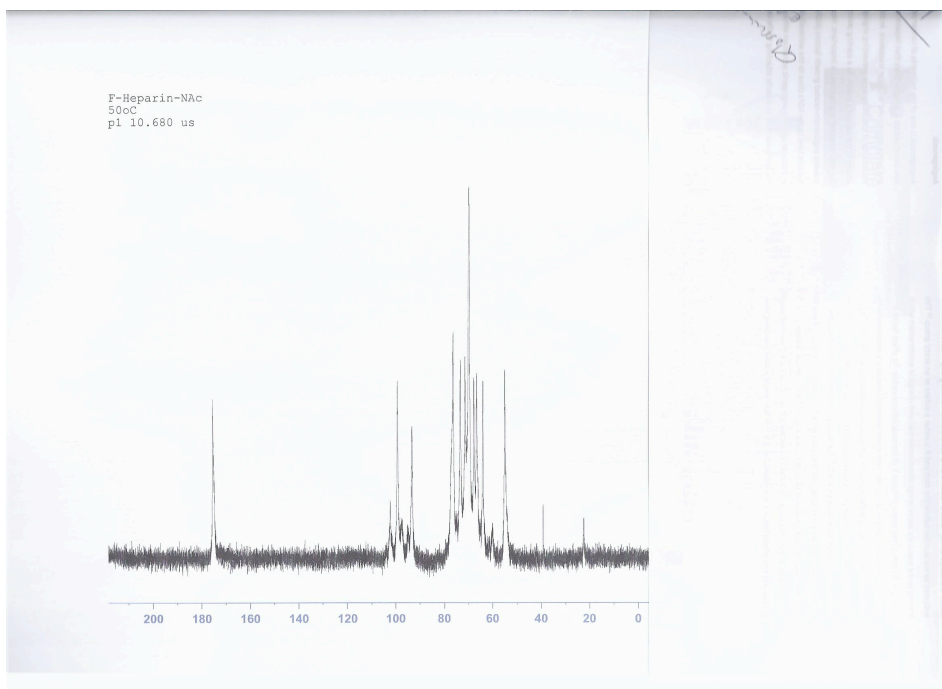
372 <sup>a</sup> Recorded at 298 K on a 500 MHz Bruker Avance III HD NMR spectrometer with 5-mm BBO probe. Chemical  
373 shift values reported relative to TFA in D<sub>2</sub>O at ( $\delta^{19}\text{F}$ ), -75.61 ppm. The chemical shift of (1) was also measured for  
374 a range of temperatures from 288 to 333 K, showing good linearity (Data not shown).

375 <sup>b</sup> Recorded at 300 K relative to trifluoroethylamine (TFEA) at ( $\delta^{19}\text{F}$ ), -65.12 ppm.  
376  
377  
378  
379  
380

381

382

383 **Supplementary Figure 1**



384

385 **Supp. Fig. 1.**  $^{13}\text{C}$  NMR spectrum of *N*-trifluoroacetyl heparin (**1**) at 50 C in  $\text{D}_2\text{O}/\text{H}_2\text{O}$

386

387 **Supplementary Figure 2**

388

389

390

391

392

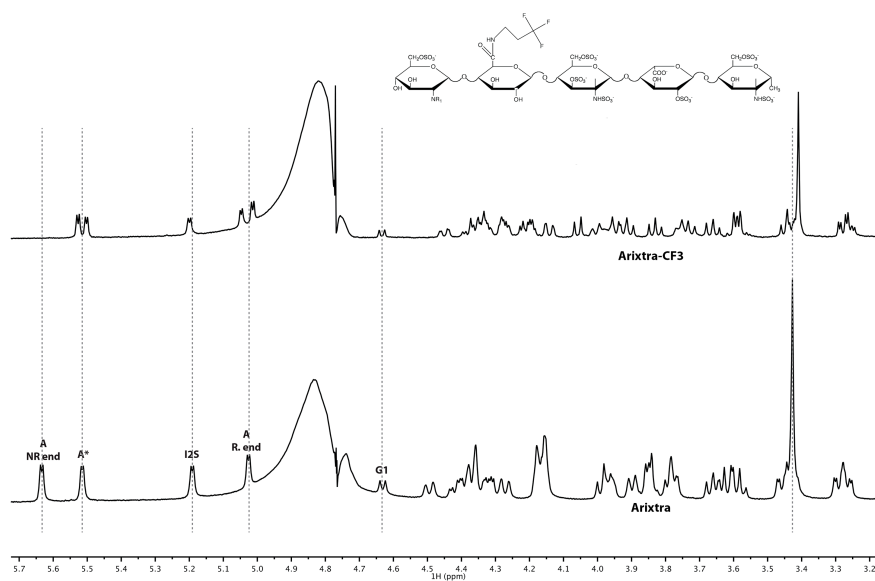
393

394

395

396

397



398 **Supp. Fig. 2.**  $^1\text{H}$  NMR spectra of AGAIA (**bottom**) and AGAIA-CF3 (**top**) at 30 °C in  $\text{D}_2\text{O}$